OXFORD

BIOLOGY Methods & Protocols

Biology Methods and Protocols, 2023, bpad016

https://doi.org/10.1093/biomethods/bpad016

Advance Access Publication Date: 10 August 2023

Protocols

Protein-Protein and Protein-Nucleic Acid Interaction and Proteomics

An advanced protocol for profiling RNA-binding proteins in Arabidopsis using plant phase extraction

Yong Zhang,[1,2,†] Ye Xu,[3,†] Todd H. Skaggs,[1] Jorge F.S. Ferreira,[1] Xuemei Chen [4] and Devinder Sandhu [1,*]

[1]U.S. Salinity Laboratory (USDA-ARS), 450 W Big Springs Road, Riverside, CA 92507, United States

[2]Department of Environmental Sciences, University of California, Riverside, CA 92521, United States

[3]Department of Botany and Plant Sciences, Institute of Integrative Genome Biology, University of California, Riverside, CA 92521, United States

[4]School of Life Sciences, Peking-Tsinghua Joint Center for Life Sciences, Peking University, Beijing 100871, China

*Correspondence address. U.S. Salinity Laboratory (USDA-ARS), 450 W Big Springs Road, Riverside, CA 92507, USA. E-mail: devinder.sandhu@usda.gov

†Lead Co-author

Abstract

RNA-binding proteins (RBPs) are key players in regulating cell fate and essential developmental processes. Systematic profiling of the RNA-binding proteome (RBPome) is thus indispensable for researchers aiming to understand the mechanisms of post-transcriptional gene regulation. RBPome identification methods developed in humans, mice, and bacteria have successfully identified RBPomes in these organisms. However, the biochemical and genetic complexities of plant tissues have greatly hindered the effectiveness of these methods in plants. Moreover, plant RBPs have been predominantly discovered through oligo d(T) based affinity purification (RNA-interactome capture). Since polyadenylated RNA only accounts for less than 5% of the total RNA population in eukaryotic cells, there is a pressing need to develop a comprehensive, yet unbiased, method to capture the full spectrum of RBPs in plants. Here, we describe a detailed protocol of Plant Phase Extraction (PPE), a recently developed method to identify RBPs in Arabidopsis (Zhang Y, Xu Y, Skaggs TH, *et al*. Plant phase extraction: a method for enhanced discovery of the RNA-binding proteome and its dynamics in plants. *Plant Cell* 2023; **35**: 2750–72.) [1]. The PPE method enables the efficient enrichment of both poly(A) and non-poly(A) RBPs from various tissues quickly and reproducibly. Most importantly, PPE allows for unveiling dynamic RBP–RNA interactions under various abiotic and biotic stress conditions and during different plant developmental stages. This provides a much broader and more accurate understanding of plant RBPs, marking a significant advancement in plant molecular biology.

Keywords: RNA-binding protein; protein-RNA interaction; Arabidopsis; phase extraction

Introduction

RNA-binding proteins (RBPs) are integral to virtually every aspect of RNA metabolism, from RNA maturation to degradation, modification, transport, and translation [2, 3]. Over the decades, studies have implicated that the malfunction of RBPs leads to neurodegenerative diseases, cancer, and metabolic disorders in humans [4–10]. In plants, defective RBPs have been linked to delayed flowering time, impaired ovule development, abnormal circadian rhythms, and altered stress/immune responses [11–21]. While it is crucial to understand how each RBP regulates developmental processes and responses to environmental cues, comprehensive identification of RBPs and understanding their interaction with RNA is equally, if not more, important. Such an approach will expand the current RBP repertoire and pave the way for a better understanding of RBP functions.

Traditionally, RBPs were predicted based on the sequence homology of conserved RNA-binding domains (RBDs) across species. However, proteins lacking classical RBDs, such as thymidylate synthase, aconitase, and glyceraldehyde 3-phosphate dehydrogenase (GAPDH), have been shown to bind RNAs [22–24], suggesting that computational predictions may have resulted in significant underestimation of the actual number of RBPs. In response to this, RNA interactome capture (RIC), a game-changing method based on UV-crosslinking and oligo(dT) selection, was developed to systematically capture the RNA-binding proteome (RBPome) associated with polyadenylated (poly(A)) RNAs in the cells of humans (1914 RBPs), mice (1393 RBPs), yeast (1273 RBPs), Drosophila (777 RBPs), and nematodes (594 RBPs) [25–34]. RIC was subsequently improved and applied to Arabidopsis etiolated seedlings, mesophyll protoplasts, leaves, root cell cultures, and seeds [35–40], leading to the discovery of 2782 RBPs [40, 41].

Despite its breakthroughs, RIC presents a notable limitation: it exhibits a strong bias toward RBPs that bind poly(A) RNAs. Since poly(A) RNAs/mRNA only represents a tiny fraction of total RNA in eukaryotic cells (<5%), RBPs interacting with the vast majority of non-poly(A) RNAs are very likely missing from RIC. Recently, an alternative strategy using phase separation/extraction has been introduced as a promising solution to this bias issue. This technique recovers RBPs, solely based on their physicochemical properties when in conjunction with RNAs after UV-crosslinking

[42–44]. In this method, the crosslinked RBP–RNA adducts remain in the insoluble interphase, enabling them to be separated from the free RNA in the aqueous phase and proteins in the organic phase post-acid guanidinium thiocyanate–phenol (Trizol reagent)–chloroform phase extraction. Notably, this method enables the identification of RBPs irrespective of their RNA type, unveiling hundreds of new ones that likely interact with non-poly(A) RNAs in human cell lines, mouse brains, and bacteria [42–44]. However, when applied to Arabidopsis, this method encountered challenges, likely attributed to the complex nature of plant tissues, and resulted in less-than-optimal outcomes [45].

Recently, we refined the phase extraction approach and developed Plant Phase Extraction (PPE), a method specifically designed for the enrichment of RBPs in Arabidopsis. This method retains the core concept of phase extraction employed in other organisms while introducing customized adaptations for handling complex plant tissue samples [1]. We incorporated crucial steps such as lysis, clearing, and multiple rounds of phase extraction to eliminate non-RBP contaminants. A notable example is histone H4, which was mistakenly identified as a potential RBP in a previous study that employed phase extraction without customizing the technique to the unique characteristics of plant tissues [45]. This strategy enhanced the signal-to-noise ratio, significantly improving the method's efficiency. We successfully uncovered 2517 RBPs from Arabidopsis leaf and root tissues under normal and saline conditions, including tissue-specific and salt-responsive RBPs. Nearly half of the discovered RBPs are novel and likely non-ploy(A) RBPs. Here, we present a detailed PPE protocol to aid researchers in their pursuit of enriching RBPs in plant species.

Materials and methods

Reagents, antibodies, and equipment

Murashige and Skoog (MS) basal medium powder (RPI, Catalog number: M10200-50.0)
Sucrose (Sigma-Aldrich, Catalog number: S0389-5KG)
Agar (RPI, Catalog number: A20400-1000.0)
Chlorox (The Chlorox Company, Catalog number: USA001067)
1 M Tris–HCl buffer, pH 7.5 (Thermo Fisher Scientific, Catalog number: 15567027)
8 M Lithium chloride solution (Sigma-Aldrich, Catalog number: L7026-100ML)
Lithium dodecyl sulfate (Sigma-Aldrich, Catalog number: L4632-50G)
Sodium dodecyl sulfate (Sigma-Aldrich, Catalog number: L3771-1KG)
IGEPAL CA630 (Sigma-Aldrich, Catalog number: I8896-100ML)
Polyvinylpyrrolidone 40 (Sigma-Aldrich, Catalog number: PVP40-100G)
DTT (Sigma-Aldrich, Catalog number: D0632-10G)
EDTA-free protease inhibitor cocktail (Sigma-Aldrich, Catalog number: 11836170001)
Ribonucleoside Vanadyl Complex (NEB, Catalog number: S1402S)
Trizol (Thermo Fisher Scientific, Catalog number: 15596018)
Chloroform (Thermo Fisher Scientific, Catalog number: 14-650-209)
DNase I (NEB, Catalog number: M0303L)
RiboLock RNase inhibitor (Thermo Fisher Scientific, Catalog number: FEREO0381)
Glycogen (Thermo Fisher Scientific, Catalog number: FERE0551)
Nuclease-free water (Thermo Fisher Scientific, Catalog number: AM9938)
2'-propanol (Thermo Fisher Scientific, Catalog number: 041463-K7)
Ethanol (Decon Labs, Catalog number: 2716)
Sodium chloride (Sigma-Aldrich, Catalog number: S3014-5KG)
Anti-AGO1 antibody (RRID: AB_2224930)
Anti-Histone H3 (RRID: AB_10750790)
Anti-Histone H4 (RRID: AB_296888)
Anti-HLP1 (gift from Dr. Xiaofeng Cao, Institute of Genetics and Developmental Biology, China)
Anti-Fib1/2 (gift from Dr. Xiaofeng Cao, Institute of Genetics and Developmental Biology, China)
Hoefer UVC500 Crosslinker (Hoefer, Inc.)
Gel loading tips (Genesee, Catalog number: 24-113)

Buffer recipes

1. Lysis buffer: 20 mM Tris–Cl, pH 7.5, 0.5 M LiCl, 0.5% LiDS, 0.4% IGEPAL CA630, 2.5% polyvinylpyrrolidone 40, 5 mM DTT, 10 mM Ribonucleoside Vanadyl Complex, 1.5× Roche EDTA-free protease inhibitor
2. Low SDS buffer: 50 mM Tris–Cl, pH 7.5, 1 mM EDTA, and 0.1% SDS
3. High SDS buffer: 50 mM Tris–Cl, pH 7.5, 1 mM EDTA, and 0.5% SDS

Plant materials

Wild-type *Arabidopsis thaliana* (Columbia-0) was used.

1. Seeds are surface sterilized by soaking in 50% bleach (Clorox) for 5 min and rinsed with sterilized water four times to remove the bleach.
2. Seeds are then stratified at 4°C for 3 days, sown on the MS (pH 5.8) medium containing 1% (v/w) sucrose and 0.8% (w/v) agar in two rows, and grown at 23°C under long-day conditions for 12 days with a light intensity of 120 μmol/m^2 (bulb: Philips Master TL5 HO 54W/840 SLV/40).
   Note: Plates are placed vertically in the growth chamber to facilitate the transfer of seedlings and the separate collection of roots and leaves.

UV-crosslinking of Arabidopsis tissues

1. Leaves and roots from Arabidopsis are collected and transferred separately to new 150 mm Petri dishes containing ice-cold liquid MS medium (pH 5.8), respectively.
   Note: Plant tissues and the Petri dishes should be kept in a pre-chilled buffer and on ice, respectively, to avoid degradation of protein and RNA caused by heat during the whole UV-crosslinking process.
2. Leaves are irradiated twice on the adaxial side and once on the abaxial side at 400 mJ/cm^2 in the Hoefer UVC500 Crosslinker (254 nm wavelength) with a 1-min interval between each crosslinking. Roots are crosslinked three times without flipping using the same UV dosage. Non-crosslinking control samples (noCL) are soaked in ice-cold liquid MS for approximately the same time as the crosslinked samples (CL).
   Notes: Leaf tissue, which harbors pigments such as chlorophyll, is more resistant to UV light in comparison to root tissue. Therefore, root tissue could require fewer cross-linking rounds or a lower UV intensity or duration than leaf tissue. However, our initial study maintained identical UV-crosslinking conditions for both tissues. This was to ensure

a standardized approach that would facilitate direct comparisons between the two tissue types.

3. Once the crosslinking is done, noCL and CL tissues are rinsed three times using ice-cold Tris-Cl buffer (20 mM, pH 7.5) and quickly dried with layers of paper towel. The samples can be either snap-frozen in liquid nitrogen, stored at −80°C, or processed directly.
   Notes: In our case, the samples were soaked in MS buffer during UV-crosslinking, therefore, we used higher UV intensity (400 mJ/cm^2) to counteract the negative effect on UV penetration caused by the liquid. Lower UV intensity can be applied in other studies where samples are crosslinked directly on ice without being soaked in a buffer [35, 36, 39]. Always remember that the optimal UV-crosslinking conditions should be carefully evaluated by monitoring the recovery of RBP and/or RNAs.

PPE procedures

Notes: The overview scheme of the PPE protocol is shown in Fig. 1. A five-round phase extraction, in our case, was ideal for removing non-RBP contaminants histone H3 and H4. However, we strongly recommend a pre-determination of the optimal number of rounds of PPE if PPE is practiced in different tissues or other species. The following procedures are carried out at 4°C unless specified.

1. Grind the leaf and root tissues into fine powder in liquid nitrogen using a mortar and pestle.
2. Resuspend the powder with lysis buffer (Two volumes of lysis buffer per gram of powder. 'In our study, 4 and 2 ml of lysis buffer were added into 2 g of powdered leaf tissue and 1 g of powdered root tissue, respectively'). Homogenize the cell suspension by rotating the tubes at 4°C for 30 minutes.
   Notes: From experience, 1 g of powdered tissue is sufficient for mass spectrometry analyses. We recommend starting from less tissue samples (0.2–0.5 g) for immunoblot analysis to test whether this method works.
3. Spin down tissue debris at 10 000 *g* for 15 min. Transfer the supernatant to a new tube and centrifuge at 10 000 *g* for 15 min. Transfer the cleared supernatant to a 50 ml tube. Save 200 µl of lysate as input for the following silver staining and immunoblot analysis.

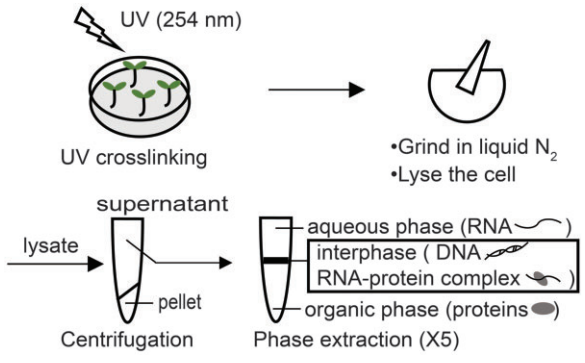

Figure 1: Schematic workflow of PPE. Samples are UV-crosslinked, ground in liquid nitrogen into a fine powder, and lysed with lysis buffer. Crude cell lysate is further cleared by centrifugation. The supernatant is collected and subjected to five rounds of phase extraction using Trizol and chloroform. RBPs associated with RNAs (in the insoluble interphase) are separated from free RNAs (in the aqueous phase) and proteins (in the organic phase).

Note: To minimize non-RBP contamination, it's critical to lyse and remove the cell debris by centrifugation at this step.

4. Mix the rest (~4 ml from leaf and 2 ml from root samples) with Trizol (20 ml for leaf and 10 ml for root samples), vortex vigorously for 15 s, and let sit at room temperature (RT) for 5 min. This process disrupts protein–protein interactions and ensures that RBP–RNA adducts are free of non-RBP contaminants.
5. Add chloroform (4 ml for leaf and 2 ml for root sample) and vigorously vortex the mixture for 15 s. Incubate the mixture at RT for 5 min.
6. Centrifuge the tubes at 10 000 *g* for 15 min to form three phases: the aqueous phase, the interphase, and the organic phase (first round of phase extraction).
   Notes: The insoluble interphase contains much fewer contaminants after introducing the lysis and pre-clearance steps (steps 2 and 3) when compared with samples directly lysed with trizol without spinning down the cell debris (Fig. 2).
7. Sequentially remove the aqueous and organic phases by pipetting with gel loading tips ('low retention tips are strongly recommended') or a syringe with a narrow needle (30G). Centrifuge the tube containing the interphase at 10 000 *g* for 5 min and remove the residual aqueous and organic phases.
   Notes: It's normal to carry residual contaminants from the aqueous and the organic phases. Be careful not to agitate the interphase when transferring the aqueous and the organic phases.
8. Add 1 ml of Trizol to the interphase and vortex for 15 s. Incubate at RT for 5 min.
9. Add 200 µl of chloroform to the tube and vortex for 15 s. Let sit for 2 min at RT.

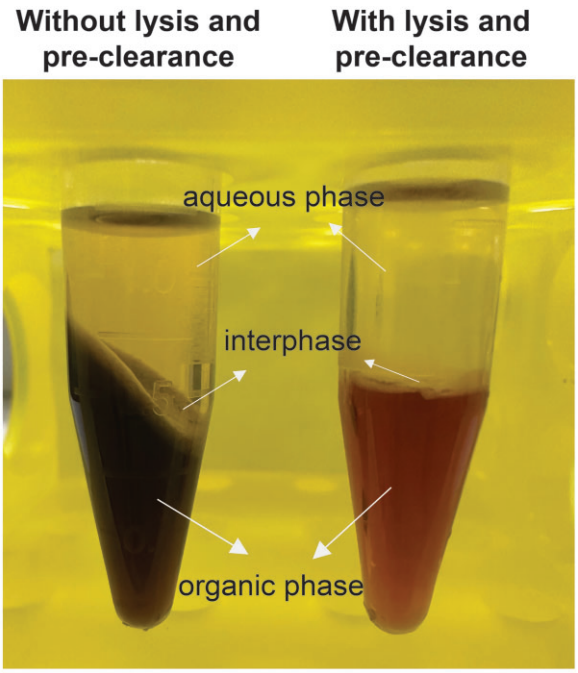

Figure 2: Comparison of phases. Phases from the sample lysed directly with Trizol (left) and lysed with lysis buffer and pre-cleared by centrifugation (right) are shown after the Trizol–chloroform phase separation. A thicker, solid interphase with cell debris can be seen on the left.

10. Centrifuge the tube at 10 000 *g* for 15 min to form phases again ('second round of phase extraction').
11. Repeat steps 7–10 as the third round of phase extraction.
12. Repeat step 7 to separate the interphase.
13. Slowly add 1 ml of 2′-propanol to the tube (avoid disrupting the interphase). Gently flip the tube upside down.
14. Centrifuge the tube at 14 000 *g* for 5 min to pellet down the interphase, then discard the supernatant.
15. Rinse the pellet with 1 ml of 70% ethanol and centrifuge the tube at 14 000 *g* for 5 min to pellet down the interphase and discard the supernatant.
16. Repeat step 15.
17. Air dry the pellet, then resuspend the pellet in 300 µl of low SDS buffer by pipetting.
18. Centrifuge the tube at 14 000 *g* for 5 min. Save the supernatant as eluate 1, and place the tube on ice.
19. Resuspend the pellet again with 300 µl of low SDS buffer by pipetting.
20. Centrifuge the tube at 14 000 *g* for 5 min, and save the supernatant as eluate 2.
21. Add 300 µl of high SDS buffer to resuspend the pellet, then centrifuge the tube at 14 000 *g* for 5 min. Save the supernatant as eluate 3, and place it on ice.
22. Resuspend the pellet with 300 µl of high SDS buffer, and centrifuge the tube at 14 000 *g* for 5 min. Transfer the supernatant and merge with all the other three eluates.
23. Sequentially add 2 µl of glycogen, 1/10 volume of 5M NaCl (~120 µl), and nine volumes of ethanol (~12 ml) to the eluates. Leave the tube at −80°C for a duration ranging from 2 h up to overnight.
24. Spin down the RBP–RNA adducts at maximum speed for 30 min.
25. Rinse the pellet with 1 ml of 70% ethanol, spin down the pellet at 14 000 *g* for 5 min, and discard the supernatant.
26. Repeat step 25.
27. Air dry the pellet ('Don't overdry it').
28. Add 200 µl of RNase-free water to resuspend the pellet. Incubate on ice for 1 h with occasional gentle pipetting to completely dissolve the pellet.
29. Add 50 µl of DNase I mixture (25 µl of 10× DNase I buffer, 18 µl of NEB DNase I, 2 µl of 1 M DTT, and 5 µl of RiboLock RNase inhibitor) to the solution and incubate at 37°C for 30 min.
30. Add 1 ml of Trizol to the interphase and vortex for 15 s. Incubate at RT for 5 min.
31. Add 200 µl of chloroform to the tube and vortex for 15 s. Let it sit for 2 min at RT.
32. Centrifuge the tube at 10 000 *g* for 15 min to separate the interphase from the aqueous and the organic phases.
33. Carefully remove the aqueous and the organic phases.
34. Centrifuge the tube at 10 000 *g* for 5 min, and remove the residual aqueous and organic phases ('fourth round of phase extraction').
35. Repeat steps 30–34 for a fifth round of phase extraction.
36. Repeat steps 13–15 to wash away the residual aqueous and organic phases.
37. Briefly air dry the pellet ('Don't overdry it').
38. Add 80 µl of 1× SDS sample buffer to resuspend the pellet. Denature the proteins by heating them at 99°C for 10 min. Then the sample is ready for downstream experiments. For silver staining, 5 µl of 20-fold diluted Input and 1 µl of denatured interphase proteins from CL and noCL samples were used; for immunoblot, 8 µl of denatured input and interphase proteins from CL and noCL samples were used (Fig. 3). The remaining samples (40–50 µl) were used for mass spectrometry analyses.

    Note: Instead of being denatured immediately, the RBP-RNA complexes from step 37 can also be recovered by repeating steps 17–28, and treated with RNase or proteinase to recover RBP or RNA, respectively.

Discussion

Although the phase extraction-based method has been successfully applied in human cells, mouse brains, and bacteria, the performance of such an approach in plants is far from satisfactory [45]. We observed a much more complex interphase without optimizing the protocol used in other organisms to suit plant tissues.

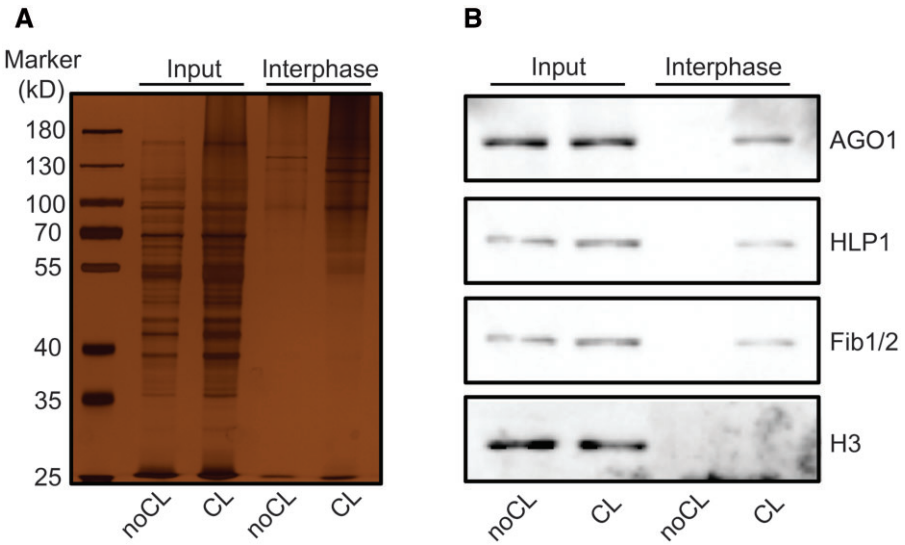

Figure 3: Comparison of interphases between noCL and CL samples. (A) Silver staining of the root total protein (shown as "Input") and the proteins in the interphase from the CL and the noCL samples of root tissue. (B) Immunoblot results show the enrichment of three RBPs (AGO1, HLP1, and Fib1/2), but not the non-RBP contaminant histone H3, in the CL root tissue.

In this interphase, RBP–RNA adducts are embedded with secondary metabolites, starch, and other substances tightly associated with cell debris. These unwanted elements likely contributed to the poor recovery of *bona fide* RBPs and overrepresented non-RBP contaminants.

We developed the PPE method to counter these challenges. The PPE protocol introduces a lysis step followed by centrifugation to clear the cell lysate, a procedure not originally included in the standard phase extraction process. Additionally, PPE features multiple rounds of biphasic separations, further improving the separation and identification of genuine RBPs. We have validated the robustness and versatility of PPE in capturing the RBPome in Arabidopsis [1]. When compared to the earlier use of a similar phase extraction-based technique in Arabidopsis [orthogonal organic phase separation (OOPS)] [43], PPE markedly outperformed by capturing a significantly larger and more reliable set of RBPs (2517 versus 468) [1]. Additionally, PPE demonstrated greater overlap with each individual RIC RBPome, exhibiting 47%–73% overlap with RIC, as opposed to the mere 7%–18% overlap demonstrated between RIC and OOPS. Moreover, PPE surpassed the RIC studies in terms of the total quantity and diversity of RBPs and RBDs [1]. The standout feature of PPE is its capacity to identify RBPs irrespective of RNA type. Within the dataset obtained by PPE (PPE-RBPome), almost half of the RBPs (1219) were previously unidentified in comprehensive RIC studies, which spanned a wide variety of cell/tissue types and developmental stages focusing on poly(A) RNA RBPs [1]. Of these newly identified 1219 RBPs, 1169 are not included in either the RIC-RBPomes or the OOPS-RBPome. This clearly illustrates the exceptional capability of PPE in discovering novel RBPs [1].

The true strength of the PPE method lies in its broad adaptability. It can be used with minimal or no modification to identify RBPs across various complex tissues and other plant species. Furthermore, it can detect RBP–RNA dynamics under a range of conditions, from normal plant growth to stress conditions and during different developmental transitions. The PPE method is an effective tool for expanding our understanding of RBPs and their critical roles in plant biology.

Acknowledgements

The authors thank Dr. Xiaofeng Cao (Institute of Genetics and Developmental Biology, Chinese Academy of Sciences) for providing anti-HLP1 and anti-Fib1/2 antibodies and Dr. Haiyan Zheng for mass-spectrometry analyses (Center for Advanced Biotechnology and Medicine, Rutgers University).

Disclaimer

The use of trade, firm, or corporation names in this publication is for the information and convenience of the reader. Such use does not constitute an official endorsement or approval by the US Department of Agriculture or the Agricultural Research Service of any product or service to the exclusion of others that may be suitable.

Author contributions

Yong Zhang (Conceptualization [equal], Data curation [lead], Formal analysis [lead], Investigation [equal], Methodology [lead], Writing—original draft [equal]), Ye Xu (Formal analysis [equal], Investigation [equal], Writing—review & editing [equal]), Todd H. Skaggs (Supervision [equal], Writing—review & editing [equal]), Jorge F.S. Ferreira (Supervision [equal], Writing—review & editing [equal]), Xuemei Chen (Conceptualization [equal], Supervision [equal], Writing—review & editing [equal]), and Devinder Sandhu (Conceptualization [equal], Formal analysis [equal], Funding acquisition [equal], Project administration [equal], Resources [equal], Supervision [equal], Writing—review & editing [equal])

Conflict of interest statement

The authors declare no conflict of interest.

Funding

This research was funded by the US Department of Agriculture-Agricultural Research Service, National Program 301: Plant Genetic Resources, Genomics, and Genetic Improvement (project number 2036-13210-013-000D), National Program 211: Water Availability & Watershed Management (project number 2036-61000-019-000D), and the National Institute of Food and Agriculture (project number CA-R-BPS-5084-H). The funders had no role in the design of the study, in the collection, analyses, or interpretation of data, in the writing of the manuscript, or in the decision to publish the results.

Data availability

Raw Mass-spectrometry data are deposited in the UCSD MassIVE database under the Identifier MSV000091682 (https://massive.ucsd.edu/ProteoSAFe/static/massive.jsp).

References

1. Zhang Y, Xu Y, Skaggs TH, *et al.* Plant phase extraction: a method for enhanced discovery of the RNA-binding proteome and its dynamics in plants. *Plant Cell* 2023;**35**:2750–72.
2. Glisovic T, Bachorik JL, Yong J *et al.* RNA-binding proteins and post-transcriptional gene regulation. *FEBS Lett* 2008;**582**:1977–86.
3. Singh G, Pratt G, Yeo GW *et al.* The clothes make the mRNA: past and present trends in mRNP fashion. *Annu Rev Biochem* 2015;**84**:325–54.
4. Gebauer F, Schwarzl T, Valcárcel J *et al.* RNA-binding proteins in human genetic disease. *Nat Rev Genet* 2021;**22**:185–98.
5. Wang X, Liu R, Zhu W *et al.* UDP-glucose accelerates SNAI1 mRNA decay and impairs lung cancer metastasis. *Nature* 2019;**571**:127–31.
6. Bechara EG, Sebestyén E, Bernardis I *et al.* RBM5, 6, and 10 differentially regulate NUMB alternative splicing to control cancer cell proliferation. *Mol Cell* 2013;**52**:720–33.
7. Louis JM, Agarwal A, Aduri R *et al.* Global analysis of RNA–protein interactions in TNF-alpha induced alternative splicing in metabolic disorders. *FEBS Lett* 2021;**595**:476–90.
8. Patel A, Lee HO, Jawerth L *et al.* A liquid-to-solid phase transition of the ALS protein FUS accelerated by disease mutation. *Cell* 2015;**162**:1066–77.
9. Verkerk AJ, Pieretti M, Sutcliffe JS *et al.* Identification of a gene (FMR-1) containing a CGG repeat coincident with a breakpoint cluster region exhibiting length variation in fragile X syndrome. *Cell* 1991;**65**:905–14.

10. Lefebvre S, Bürglen L, Reboullet S *et al.* Identification and characterization of a spinal muscular atrophy-determining gene. *Cell* 1995;**80**:155–65.
11. Bush MS, Crowe N, Zheng T *et al.* The RNA helicase, eIF4A-1, is required for ovule development and cell size homeostasis in Arabidopsis. *Plant J* 2015;**84**:989–1004.
12. Macknight R, Bancroft I, Page T *et al.* FCA, a gene controlling flowering time in Arabidopsis, encodes a protein containing RNA-binding domains. *Cell* 1997;**89**:737–45.
13. Schomburg FM, Patton DA, Meinke DW *et al.* FPA, a gene involved in floral induction in Arabidopsis, encodes a protein containing RNA-recognition motifs. *Plant Cell* 2001;**13**:1427–36.
14. Zhang Y, Gu L, Hou Y *et al.* Integrative genome-wide analysis reveals HLP1, a novel RNA-binding protein, regulates plant flowering by targeting alternative polyadenylation. *Cell Res* 2015;**25**:864–76.
15. Heintzen C, Nater M, Apel K *et al.* AtGRP7, a nuclear RNA-binding protein as a component of a circadian-regulated negative feedback loop in *Arabidopsis thaliana*. *Proc Natl Acad Sci USA* 1997;**94**:8515–20.
16. Marondedze C, Thomas L, Lilley KS *et al.* Drought stress causes specific changes to the spliceosome and stress granule components. *Front Mol Biosci* 2019;**6**:163.
17. Albaqami M, Laluk K, Reddy ASN. The Arabidopsis splicing regulator SR45 confers salt tolerance in a splice isoform-dependent manner. *Plant Mol Biol* 2019;**100**:379–90.
18. Kim YO, Kim JS, Kang H. Cold-inducible zinc finger-containing glycine-rich RNA-binding protein contributes to the enhancement of freezing tolerance in *Arabidopsis thaliana*. *Plant J* 2005;**42**:890–900.
19. Zhang Y, Cheng YT, Bi D *et al.* MOS2, a protein containing G-patch and KOW motifs, is essential for innate immunity in *Arabidopsis thaliana*. *Curr Biol* 2005;**15**:1936–42.
20. Deleris A, Gallego-Bartolome J, Bao J *et al.* Hierarchical action and inhibition of plant Dicer-like proteins in antiviral defense. *Science* 2006;**313**:68–71.
21. Zhang X, Zhao H, Gao S *et al.* Arabidopsis Argonaute 2 regulates innate immunity via miRNA393 (-)mediated silencing of a Golgi-localized SNARE gene, MEMB12. *Mol Cell* 2011;**42**:356–66.
22. Chu E, Koeller DM, Casey JL *et al.* Autoregulation of human thymidylate synthase messenger RNA translation by thymidylate synthase. *Proc Natl Acad Sci USA* 1991;**88**:8977–81.
23. Hentze MW, Argos P. Homology between IRE-BP, a regulatory RNA-binding protein, aconitase, and isopropylmalate isomerase. *Nucleic Acids Res* 1991;**19**:1739–40.
24. Chang CH, Curtis JD, Maggi LB *et al.* Posttranscriptional control of T cell effector function by aerobic glycolysis. *Cell* 2013;**153**:1239–51.
25. Kwon SC, Yi H, Eichelbaum K *et al.* The RNA-binding protein repertoire of embryonic stem cells. *Nat Struct Mol Biol* 2013;**20**:1122–30.
26. Beckmann BM, Horos R, Fischer B *et al.* The RNA-binding proteomes from yeast to man harbour conserved enigmRBPs. *Nat Commun* 2015;**6**:10127.
27. Liao Y, Castello A, Fischer B *et al.* The cardiomyocyte RNA-binding proteome: links to intermediary metabolism and heart disease. *Cell Rep* 2016;**16**:1456–69.
28. Liepelt A, Naarmann-de Vries IS, Simons N *et al.* Identification of RNA-binding proteins in macrophages by interactome capture. *Mol Cell Proteomics* 2016;**15**:2699–714.
29. Matia-Gonzalez AM, Laing EE, Gerber AP. Conserved mRNA-binding proteomes in eukaryotic organisms. *Nat Struct Mol Biol* 2015;**22**:1027–33.
30. Sysoev VO, Fischer B, Frese CK *et al.* Global changes of the RNA-bound proteome during the maternal-to-zygotic transition in drosophila. *Nat Commun* 2016;**7**:12128.
31. Despic V, Dejung M, Gu M *et al.* Dynamic RNA-protein interactions underlie the zebrafish maternal-to-zygotic transition. *Genome Res* 2017;**27**:1184–94.
32. Hentze MW, Castello A, Schwarzl T *et al.* A brave new world of RNA-binding proteins. *Nat Rev Mol Cell Biol* 2018;**19**:327–41.
33. Castello A, Fischer B, Eichelbaum K *et al.* Insights into RNA biology from an atlas of mammalian mRNA-binding proteins. *Cell* 2012;**149**:1393–406.
34. Baltz AG, Munschauer M, Schwanhäusser B *et al.* The mRNA-bound proteome and its global occupancy profile on protein-coding transcripts. *Mol Cell* 2012;**46**:674–90.
35. Reichel M, Liao Y, Rettel M *et al.* In planta determination of the mRNA-binding proteome of arabidopsis etiolated seedlings. *Plant Cell* 2016;**28**:2435–52.
36. Marondedze C, Thomas L, Serrano NL *et al.* The RNA-binding protein repertoire of Arabidopsis thaliana. *Sci Rep* 2016;**6**:29766.
37. Zhang Z, Boonen K, Ferrari P *et al.* UV crosslinked mRNA-binding proteins captured from leaf mesophyll protoplasts. *Plant Methods* 2016;**12**:42.
38. Marondedze C, Thomas L, Gehring C *et al.* Changes in the Arabidopsis RNA-binding proteome reveal novel stress response mechanisms. *BMC Plant Biol* 2019;**19**:139.
39. Bach-Pages M, Homma F, Kourelis J, *et al.* Discovering the RNA-binding proteome of plant leaves with an improved RNA interactome capture method. *Biomolecules* 2020;**10**:661.
40. Sajeev N, Baral A, America AHP *et al.* The mRNA-binding proteome of a critical phase transition during Arabidopsis seed germination. *New Phytol* 2022;**233**:251–64.
41. Marondedze C. The increasing diversity and complexity of the RNA-binding protein repertoire in plants. *Proc Biol Sci* 2020;**287**:20201397.
42. Trendel J, Schwarzl T, Horos R *et al.* The human RNA-binding proteome and its dynamics during translational arrest. *Cell* 2019;**176**:391–403 e19.
43. Queiroz RML, Smith T, Villanueva E *et al.* Comprehensive identification of RNA-protein interactions in any organism using orthogonal organic phase separation (OOPS). *Nat Biotechnol* 2019;**37**:169–78.
44. Urdaneta EC, Vieira-Vieira CH, Hick T *et al.* Purification of cross-linked RNA-protein complexes by phenol-toluol extraction. *Nat Commun* 2019;**10**:990.
45. Liu J, Zhang C, Jia X *et al.* Comparative analysis of RNA-binding proteomes under Arabidopsis thaliana-Pst DC3000-PAMP interaction by orthogonal organic phase separation. *Int J Biol Macromol* 2020;**160**:47–54.